

Raman Mapping of Mannitol/Lysozyme Particles Produced Via Spray Drying and Single Droplet Drying

Jari Pekka Pajander · Sanni Matero · Jakob Sloth · Feng Wan · Jukka Rantanen · Mingshi Yang

Received: 8 August 2014 / Accepted: 2 December 2014 / Published online: 13 December 2014
© Springer Science+Business Media New York 2014

ABSTRACT

Purpose This study aimed to investigate the effect of a model protein on the solid state of a commonly used bulk agent in spray-dried formulations.

Methods A series of lysozyme/mannitol formulations were spray-dried using a lab-scale spray dryer. Further, the surface temperature of drying droplet/particles was monitored using the DRYING KINETICS ANALYZER™ (DKA) with controllable drying conditions mimicking the spray-drying process to estimate the drying kinetics of the lysozyme/mannitol formulations. The mannitol polymorphism and the spatial distribution of lysozyme in the particles were examined using X-ray powder diffractometry (XRPD) and Raman microscopy. Partial Least Squares Discriminant Analysis was used for analyzing the Raman microscopy data.

Results XRPD results indicated that a mixture of β -mannitol and α -mannitol was produced in the spray-drying process which was supported by the Raman analysis, whereas Raman analysis indicated that a mixture of α -mannitol and δ -mannitol was detected in the single particles from DKA. In addition Raman mapping indicated that the presence of lysozyme seemed to favor the appearance of α -mannitol in the particles from DKA evidenced by close proximity of lysozyme and mannitol in the particles.

Conclusions It suggested that the presence of lysozyme tend to induce metastable solid state forms upon the drying process.

KEY WORDS drying kinetics · lysozyme · mannitol polymorphism · Raman mapping · spray-drying · X-ray powder diffraction

INTRODUCTION

Mannitol may be one of the most commonly used pharmaceutical excipients. It is widely used as a bulk agent in tablet formulations including conventional tablets, chewable tablets and rapidly disintegrating tablets due to its good compatibility with many drugs. It is also particularly useful when formulating moisture sensitive drugs because of its non-hygroscopicity (1). Besides tablet formulations it has also been attempted in inhalable dry protein formulations (2,3). For example the first inhalable insulin product Exubera contained mannitol to stabilize insulin during the spray-drying process (4). In addition, it has been added in freeze drying protein formulations to provide a pharmaceutically acceptable cake (stable matrix structure), and serve as a stabilizer to prevent proteins from stress involved in the dehydration process (5).

Besides amorphous form, mannitol generally occurs as a crystalline and several polymorphic forms are known to exist, namely anhydrous α -, β -, and δ -mannitol as well as mannitol hemihydrate (6,7). Studies have shown that the change in the solid state form of mannitol upon processing can affect mannitol morphology (1), and protein stability (8). In general, for protein formulations, mannitol needs to be in an amorphous glass matrix to serve as a stabilizer, while crystalline mannitol is considered to be ineffective in preserving protein activity. Nevertheless this finding has so far not been further specified whether the three anhydrous polymorphs might behave differently in this regard (9). In addition, the phase separation due to recrystallization of glass state mannitol upon storage may cause degradation of proteins. Thus it will be of interest to study the interplay between protein and mannitol upon drying and storage. Moreover given the four crystalline solid

J. P. Pajander · S. Matero · F. Wan · J. Rantanen · M. Yang (✉)
Department of Pharmacy, University of Copenhagen, Universitetsparken
2, 2100 Copenhagen, Denmark
e-mail: mingshi.yang@sund.ku.dk

S. Matero
Quality and Technology, Department of Food Science, Faculty of Science
University of Copenhagen, Rolighedsvej 30, 1958 Frederiksberg
Denmark

J. Sloth
GEA Process Engineering A/S, Gladsaxevej 305, 2860 Soeborg
Denmark

forms of mannitol besides its amorphous form, mannitol can be an excellent model compound to study solid state transformation upon processing in the presence of excipients. An example can be to study how co-solutes (e.g. protein drugs or protein excipients) direct the solid state form of small molecule drugs (e.g. use mannitol as a model small molecule) upon dehydration.

Previous studies have reported that the solid forms of mannitol in spray-dried protein formulations have been found to be both process and protein related (9,10). For example, amorphous mannitol was produced when co-spray-drying of trypsin:mannitol at ratios of 1:9, 1:1 and 9:1 (*w/w*), while a mixture of β - and δ - mannitol were produced when co-spray-drying of lysozyme:mannitol at the same ratios (10). A recent study showed the prevalence of mannitol polymorphism shifted from β - mannitol to δ - mannitol with an increase in lysozyme concentration in freeze-dried formulations, while in spray-drying formulations, an increase in lysozyme concentration resulted in a shift from β - mannitol to α -mannitol (9). Further Lee *et al.* reported particle size dependence of mannitol polymorphism in the spray-dried powder (11), which implies the complex of the interplay between mannitol and proteins upon drying.

In this study, a single droplet levitation technique (12) was used to process mannitol/protein formulation and the mannitol polymorphism of the particles from this technique was compared with that from a spray-drier in order to investigate the influence of the protein on polymorphism of mannitol during the spray-drying process. The mannitol polymorphism was analyzed using X-ray powder diffractometer and Raman spectrometer. In addition Raman mapping was conducted to observe the distribution of mannitol and protein on the particles. The Raman data was processed using Partial Least Squares Discriminant Analysis (PLS-DA) in order to obtain quantitative estimations of the polymorphic transformation.

MATERIALS AND METHODS

Materials

D-Mannitol ($\geq 98.5\%$) and Chicken egg-white lysozyme crystalline powder (Product No. 62971) were purchased from VWR International Ltd., Poole, England and Fluka Analytical, respectively. Protein was stored at 4°C and mannitol powders were stored in airtight, light resistant containers at room temperature until use. Distilled water was used for the whole experiment.

Formulations containing 0, 2.5, 10 and 50% (*w/w*) of lysozyme (in terms of mannitol mass) were processed by both the spray-drying process and single droplet levitation.

Spray-drying Process

Feed solutions were prepared and spray-dried using a Büchi B-290 spray dryer (Büchi Labortechnik AG, Postfach, Switzerland) under the following operating conditions: feed concentration of 0.10 g/ml, spray air flow of 11.1 L/min, dry air flow of 0.45 m³/min, feed rate of 4.3 g/min and inlet temperature of 130°C. Outlet temperature was 55–56°C, but in the case of 10% lysozyme solution 54–55°C. The spray-dried powders were collected into glass scintillation vials, sealed with Parafilm and kept in a glass desiccators containing silica gel as drying agent at room temperature until analysis.

SEM

Scanning electron microscopy (SEM) was performed a Zeiss Ultra55 scanning electron microscope (SEM, Carl Zeiss, Denmark) to visualize the morphology of the spray dried particles. Briefly, the spray dried particles were placed on a sticky carbon tape followed by sputter coating with a 5 nm thick layer of gold to make the surfaces conductive. The specimens were then imaged at an accelerating voltage of 3 kV.

XRPD

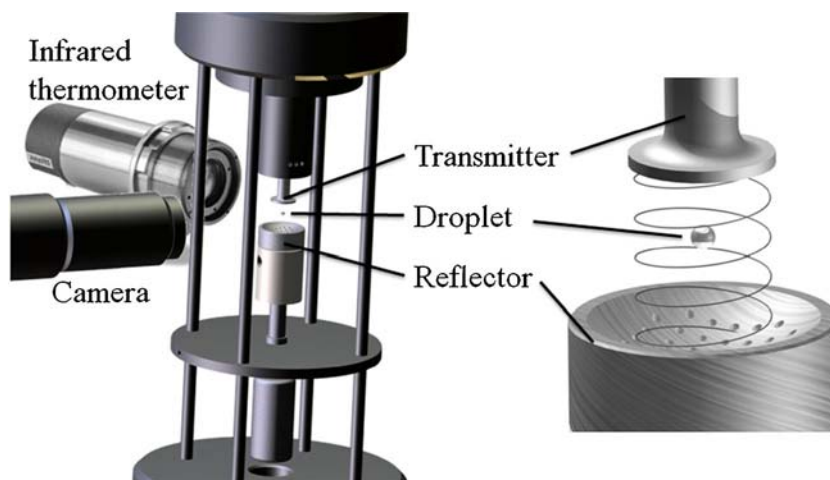
The X-Ray powder diffraction analysis was performed with PANalytical X'Pert PRO MPD (PW3040/60, Philips, Netherlands) using a copper (Cu) anode for radiation with $\lambda = 1.542 \text{ \AA}$, 45 kV and 40 mA. The samples were transferred onto a silicon plate fitted in a sample holder. The samples were measured from 5°–40° 2 θ with a step size of 0.02626° and scanning speed of 0.0673° per second.

Drying Kinetics by Single Droplet Levitation

In this study, the single droplet drying experiments were conducted using the DRYING KINETICS ANALYZER™ (DKA). The DKA is presented in detail elsewhere (13,14) and therefore only described briefly here. The apparatus (Fig. 1) consists of a levitator where a small droplet ($d \in [0.15\text{--}1.5] \text{ mm}$) may be held constant against gravity due to the forces of an ultrasonic field between the transmitter and the reflector (Fig. 1). The droplet in the ultrasonic field dries while monitored with a CCD-camera. Also, while the droplet is drying the surface temperature is continuously measured using an infrared thermometer.

The levitator is encapsulated in a small drying chamber (not shown in Fig. 1) in which the gas temperature and humidity may be arbitrary. The nitrogen drying gas is injected through small holes in the reflector below the droplet to simulate the relative velocity between the gas and droplets in a spray dryer. Further, to obtain good agreement between the course of drying in the DKA and in a spray dryer it is

Fig. 1 Left: drying kinetics analyzer™. Right: zoom on the levitated droplet where the helix illustrates the ultrasonic field. Note the holes in the reflector used to inject conditioned drying gas.



important to use the outlet temperature from the spray dryer in the DKA (14).

Polarized Microscopy

Polarized light microscopy images of single droplet levitation particles were obtained by a light microscopy (Aciolab, Carl Zeiss, Göttingen, Germany) at magnification of $5\times$. The images were recorded by a digital camera (Moticam 10.0 MO, Swift Optical Instruments Inc., Texas, USA) using a Motic image plus 2.0 software (Swift Optical Instruments Inc., Texas, USA).

Raman Mapping of Spray-Dried Powder and Particles from Single Droplet Levitation

Raman spectra acquisition of pure mannitol polymorphs and lysozyme, and Raman mapping of single droplet levitation particles and spray-dried powder, was performed by Renishaw system 1000 micro-Raman Microscope spectrometer (Renishaw plc, New Mills, UK) and by Wire V 2.0 software (Renishaw plc, New Mills, UK). Magnification of $5\times$ (spot size of approx. $8\ \mu\text{m}$) and exposure time of HPNIR diode laser (785 nm) of 10 s were used in spectra acquisition of pure compounds. The Raman mapping was performed with a magnification of $20\times$ generating a spot size of approx. $2\ \mu\text{m}$. An area of $180\ \mu\text{m} \times 180\ \mu\text{m}$ was divided into a grid of 7×7 spectra producing altogether 49 spectra from the surface of a sample. The distance, i.e. step size, between the collection points of one spectrum was $30\ \mu\text{m}$. In the case of single droplet levitation particles, the laser (785 nm) exposure time was 2×10 s, and for spray-dried powder 10 s.

Chemometrics and Data Processing

The chemometrics modeling was performed using Partial Least Squares Discriminant Analysis (PLS-DA), which is a

special case of PLS regression (15,16). The PLS-DA algorithm maximizes the covariance between \mathbf{X} (i.e. spectra) and \mathbf{Y} (i.e. class variables) data and simultaneously finds the directions of components that best estimate the class to which samples belong. Four classes corresponding to each pure mannitol polymorph and protein (lysozyme) were modeled ($n=6$ for each class). Spectra were preprocessed by Standard Normal Variate (SNV) correction and mean centered prior modeling. Spectral preprocessing prior analysis can be considered as standard procedure since scattering effect based on e.g. physical properties, sample (dis)placement, optical path length or detector (17) needs to be removed. The model was evaluated based on class specificity and sensitivity which gives the error rate of classification by the model. The random block cross validation (4 splits) was used to determine the optimum number of PLS-DA components. The final and overall 3-component PLS-DA model of all classes included the wavelength region of $714\text{--}821\ \text{cm}^{-1}$, based on judgment of selective region of all compounds. The model was predictive, since there was no classification error of any class.

Data handling and modeling were carried out using PLS-toolbox 5.8.3 (Eigenvector Research, Inc., Wenatchee, WA, USA) and MATLAB v.7.11 (The MathWorks, Inc., Natick, MA, USA). The contour plots presenting the spatial distribution of different mannitol polymorphs and lysozyme on basis of PLS-DA results were constructed by OriginPro (Version 8.6.0, OriginLab Corporation, Northampton, MA, USA). The contour plots were created directly from Cartesian coordinates and the procedure consisted of the four default step processes provided by the program, i.e. triangulation, linear interpolation, drawing of contour lines, and connecting and smoothing. The smoothing was performed with the following setup: total points increase factor of 100 and smoothing parameter of 0.001. The first parameter affects the amount of triangulation points. The higher the value, the more triangles, i.e. higher the resolution of gridding, are used in order to cover the data points by the procedure. The second parameter

designates how well the interpolated surface will pass through the data points. The used value can be regarded as non-skewing, since the value of 0 designates that no smoothing will take place.

RESULTS

Spray-dried Particles

Morphology

By investigating Fig. 2, it can be seen that spray-dried lysozyme/mannitol particles exhibited spherical shape when the concentration of lysozyme in the formulation is low, i.e. 2.5 and 10% (*w/w*), whereas the spray dried particles with 50% (*w/w*) lysozyme loading are raisin like. The surfaces of the spray-dried particles become very rough when the lysozyme concentration reaches 50% (*w/w*). As the process parameters were fixed in the study the atomized droplet size distribution were expected to be similar for the formulations, which resulted in the similar particle size distribution. Even though surface active properties of protein might result in early shell formation, the high solid concentration of 10% *w/w* in the feed seemed to prevent the droplets from breaking up easily due to thick shell formulation. It is also evidenced in SEM that the most particles retain intact and spherical.

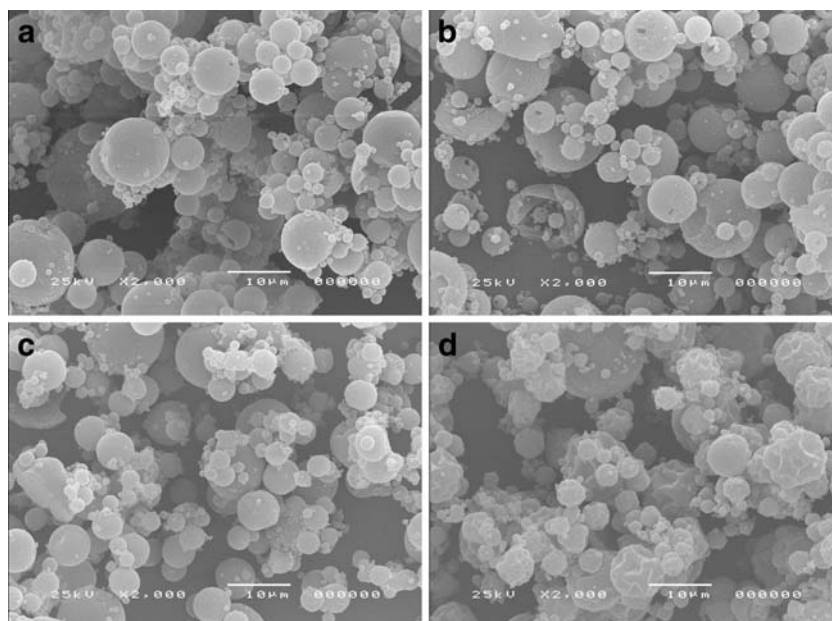
Mannitol Solid Form

The distribution of each polymorphic form of mannitol and lysozyme on the surface of the spray dried powder were

estimated with Raman mapping and PLS-DA analysis. Predicted PLS-DA scores for each sample were used as concentration estimates for each ingredient and the obtained concentration distributions were visualized as presented in Fig. 3. It can be seen that the presence of lysozyme clearly affects the solid form of mannitol. β -mannitol is the most dominating form, when lysozyme is not included in the formulation, although the results suggest that there is a small fraction of α -mannitol present. The amount of α -mannitol slightly increases as the lysozyme content is increased to 2.5% (*w/w*), however β -mannitol is still the most dominating form in the powder blend. Interestingly, there were hardly any traces of lysozyme present in the Raman signal with concentration of 2.5% (*w/w*). The ratio between α - and β -mannitol changes, when the nominal lysozyme content is 10% (*w/w*). Now the dominating form is α -mannitol, but the measured lysozyme content on the surface of the spray dried powder seem to be around 3% (*w/w*), which is less than the nominal value. Lysozyme seems to be the most dominating compound on the surface, when its nominal content is 50% (*w/w*). However, according to analysis, the content of the lysozyme is high, i.e. approximately 70% (*w/w*), which is higher than the nominal content. Additionally, lysozyme affects the mannitol polymorphism, since the presence of α -mannitol seems to increase with an increase in the lysozyme content. Finally, no traces of δ -mannitol were seen in any of the spray dried powder blend.

The findings from XRPD measurement were in agreement with the findings from Raman mapping and PLS-DA analysis. As shown in the reference XRPD pattern of mannitol in Fig. 4a α -mannitol has characteristic reflections at 13.8° and 17.3° of 2θ while intensive reflections at 14.7° and 16.8° can be attributed to β -mannitol (They were highlighted as rectangle in Fig. 4a). When the concentration of lysozyme is low (0 or

Fig. 2 SEM of spray-dried lysozyme/mannitol powder: (a), 0% (*w/w*) lysozyme; (b), 2.5% (*w/w*) lysozyme; (c), 10% (*w/w*) lysozyme; (d), 50% (*w/w*) lysozyme.



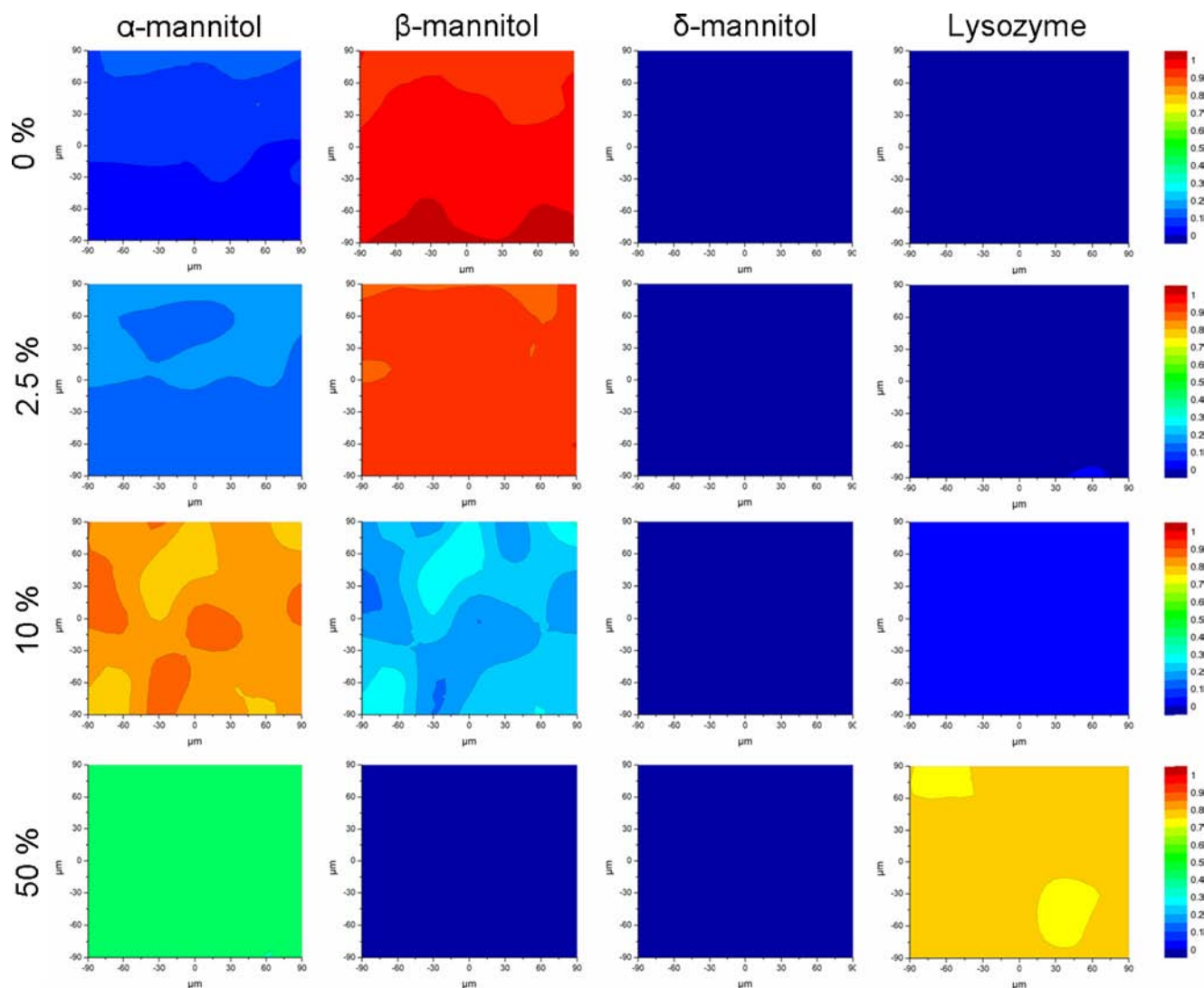


Fig. 3 The contour plots indicating the distribution of different mannitol forms and lysozyme content on the surface of the spray dried powders containing different nominal concentrations of the protein.

2.5% (w/w), only β -mannitol was observed after spray-drying of the formulations (Fig. 4b). However a mixture of α -mannitol and β -mannitol was observed when lysozyme concentration was increased to 10% (w/w) after spray-drying, and there seemed to be higher proportion of α -mannitol than β -mannitol in the mixture when comparing the intensity of the reflection peaks of α -mannitol and β -mannitol. When the concentration of lysozyme was increased to 50% (w/w), besides α - and β -mannitol, an amorphous halo was observed, which is related to the high content of protein.

Single Droplet Experiments

Drying kinetics and Morphology

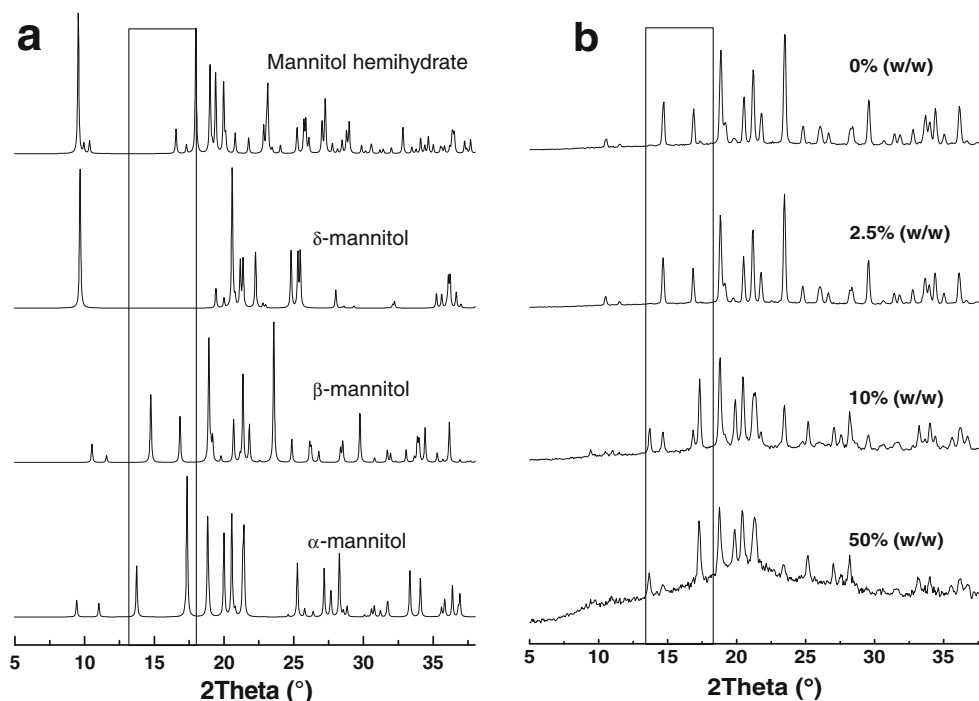
The drying kinetics of the four lysozyme formulations was studied using the DKA as described in “Drying kinetics by

single droplet levitation” section. Figure 5 shows the development in surface temperature as a function of the drying time. Note that the drying time is given as the so-called scaled time. The scaled time is the actual drying time (in seconds) divided by the squared initial droplet diameter. The initial droplet size inevitably varies between experiments but this can be compensated by using scaled time during data analysis (18).

Valuable information about the course of drying may be extracted from the surface temperature measurement, including an indication of the drying kinetics, i.e. a low surface temperature corresponding to fast drying because of evaporative cooling at the surface of the particle and contrarily a surface temperature close to that of the drying gas inlet temperature indicates a low evaporation rate corresponding to diffusion limited drying phase (19,20).

The drying profiles of the formulations consisting of low lysozyme concentration are similar to the reference

Fig. 4 XRPD pattern of spray-dried lysozyme/mannitol powder. (a), reference XRPD pattern of mannitol; (b), XRPD pattern of different formulations.



formulation (0% (*w/w*) lysozyme). While the drying of the 50% (*w/w*) lysozyme formulations exhibited different kinetics from the other formulations. It is most likely due to the accumulation of lysozyme on the surface, as proteins are generally amphiphilic and surface active. This means that the lysozyme tend to adsorb at the gas/liquid interface of the droplets which hinder transportation of water to the surface and thereby slows down the drying.

The shapes of the particles from the DKA are round as shown in Fig. 6. The increase in lysozyme content affects the morphology of mannitol crystal on the particles. The mannitol crystals are clearly visible on the surface of the particle consisting only of model excipient (Fig. 6a). The size of

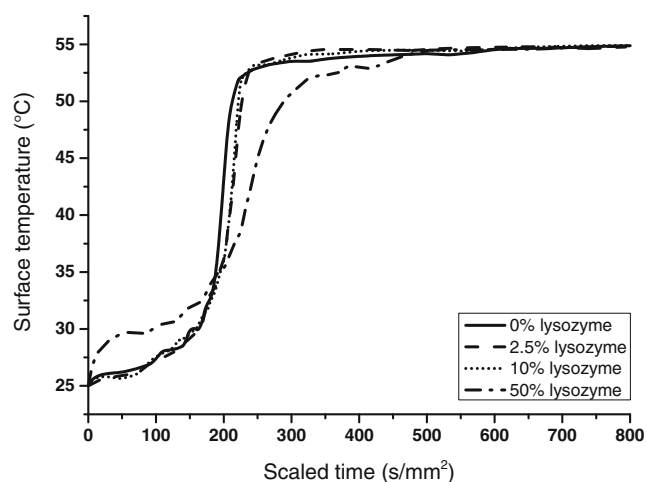


Fig. 5 Estimation of drying kinetics of the different feeds from surface temperature of the drying droplet/particle.

mannitol crystals decreases when lysozyme content is increased, while when the lysozyme content is 50% (*w/w*), the individual mannitol crystals are no longer visible on this magnification on the surface of the particle, however, the illumination due to polarized light indicates, that the content of crystalline material is high.

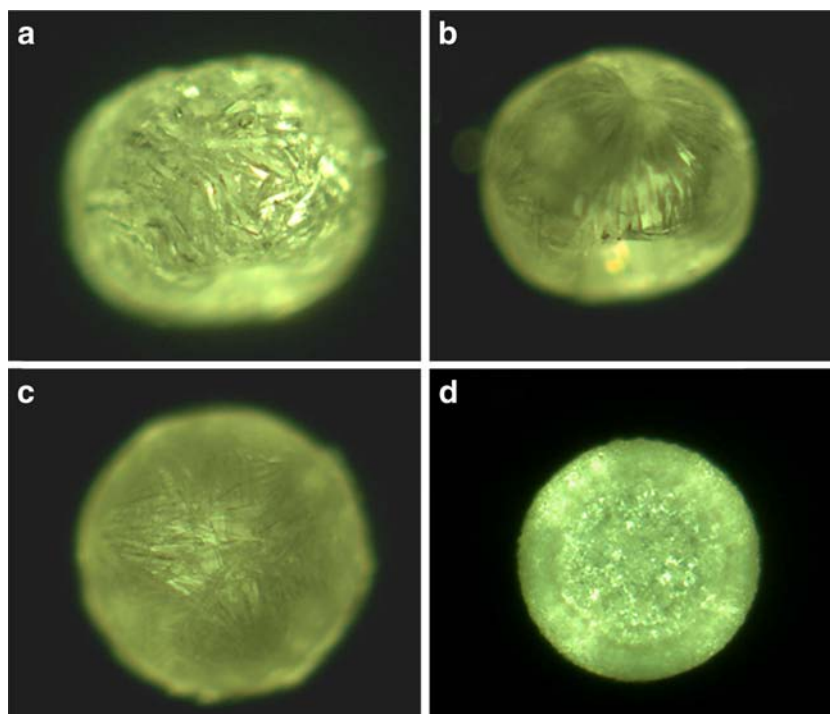
Mannitol Polymorphism in the Particles from Single Droplet Levitation

The distribution of each polymorphic form of mannitol and lysozyme on the surface of the single levitation droplet particles were estimated with the similar procedure as with spray dried powder (chapter 3.1.2). The results, which are presented in Fig. 7, indicated that the single levitation droplet particle consisted of mannitol in α - and β -forms, which of the latter seems to be slightly more dominating form as with corresponding spray dried powder. However, the distribution of different mannitol forms is not that even as with spray dried powder, and there also seems to be small traces of δ -mannitol present.

Surprisingly there is no β -mannitol present in the single droplet levitation particle, when lysozyme content is increased to 2.5% (*w/w*). In contrary to spray dried powder, this particle is consisting of α - and δ -mannitol, which of the first one seems to be more dominating form. Additionally, there is a signal of protein present corresponding to a concentration between 0 and 5% (*w/w*), but it is not evenly distributed on the surface of the particle according to PLS-DA analyses.

α -Mannitol is the most dominating polymorphic form, when the lysozyme content is increased to 10% (*w/w*),

Fig. 6 Polarized light microscopy images of single droplet levitation particles containing (a) 0% (w/w), (b) 2.5% (w/w), (c) 10% (w/w) and (d) 50% (w/w) of lysozyme.



although there also is δ -mannitol present. The protein is again unevenly distributed and there are even local protein-rich areas, where the concentration of protein is over 20% (w/w), which is twice as much as the nominal content.

Lysozyme is the most dominating compound and very evenly distributed on the surface of single droplet levitation particle, when its nominal content is 50% (w/w). However, the results indicate that the actual concentration of the protein on the surface is 60–70% (w/w). It is most likely due to the accumulation of lysozyme on the surface, as proteins are general amphiphilic and surface active, and tended to adsorb at the gas/liquid interface of the atomized droplets. Additionally, this particle seems to contain mostly α -mannitol, although there are some traces of δ -mannitol present.

Interestingly the results indicate that there is no β -mannitol present, if lysozyme is included in the formulation. Furthermore, it is notable that the presence of α -mannitol seems to be correlating with lysozyme content, which can be seen from all of the lysozyme containing single droplet levitation particles. The protein-rich areas are consisting also of α -mannitol, and δ -mannitol can be found from areas, that contain no or only a few traces of the protein.

DISCUSSION

Our recent study showed that different drying principles led to different solid state changes of mannitol in the presence of lysozyme (9). For the same formulation compositions, the

freeze-drying process resulted in a mixture of β -mannitol and δ -mannitol, and with an increase in lysozyme concentration mannitol polymorphism shifted from β -mannitol to δ -mannitol. While in the spray drying process a mixture of β -mannitol and α -mannitol were produced, and a shift from β -mannitol to α -mannitol was found with an increase in lysozyme concentration in the formulation. Some other studies on polymorphism of spray dried mannitol have reported that different proteins resulted in different solid state forms of mannitol from the spray drying process (10). Indicating mannitol polymorphism upon the spray drying process may be protein depended. In this study, DKA, a drying kinetics analyzer was employed to process lysozyme formulations with the similar drying conditions (same feed concentration, T_{outlet} and drying gas flow rate) used in the spray-drying process by Büchi Mini B-290 spray dryer. To have comparable drying conditions, mannitol/lysozyme formulations with a higher solid concentration (10% (w/w)) than the one (2% (w/w)) used in the previous study was employed, and processed by Büchi B-290 Mini spray dryer and DKA, respectively. Subsequently the mannitol polymorphism from the two processes was characterized by using XRPD and Raman spectroscopy. The Raman is also used to map the spatial distribution of lysozyme and mannitol in the particles generated from DKA.

For many years XRPD has been generally regarded as a golden standard for the polymorphic form determination from a binary mixture and their quantification. However, it is known that the method has some drawbacks, since particle size, preferred orientation and sample preparation, such as powder packing, may affect to the accuracy of the

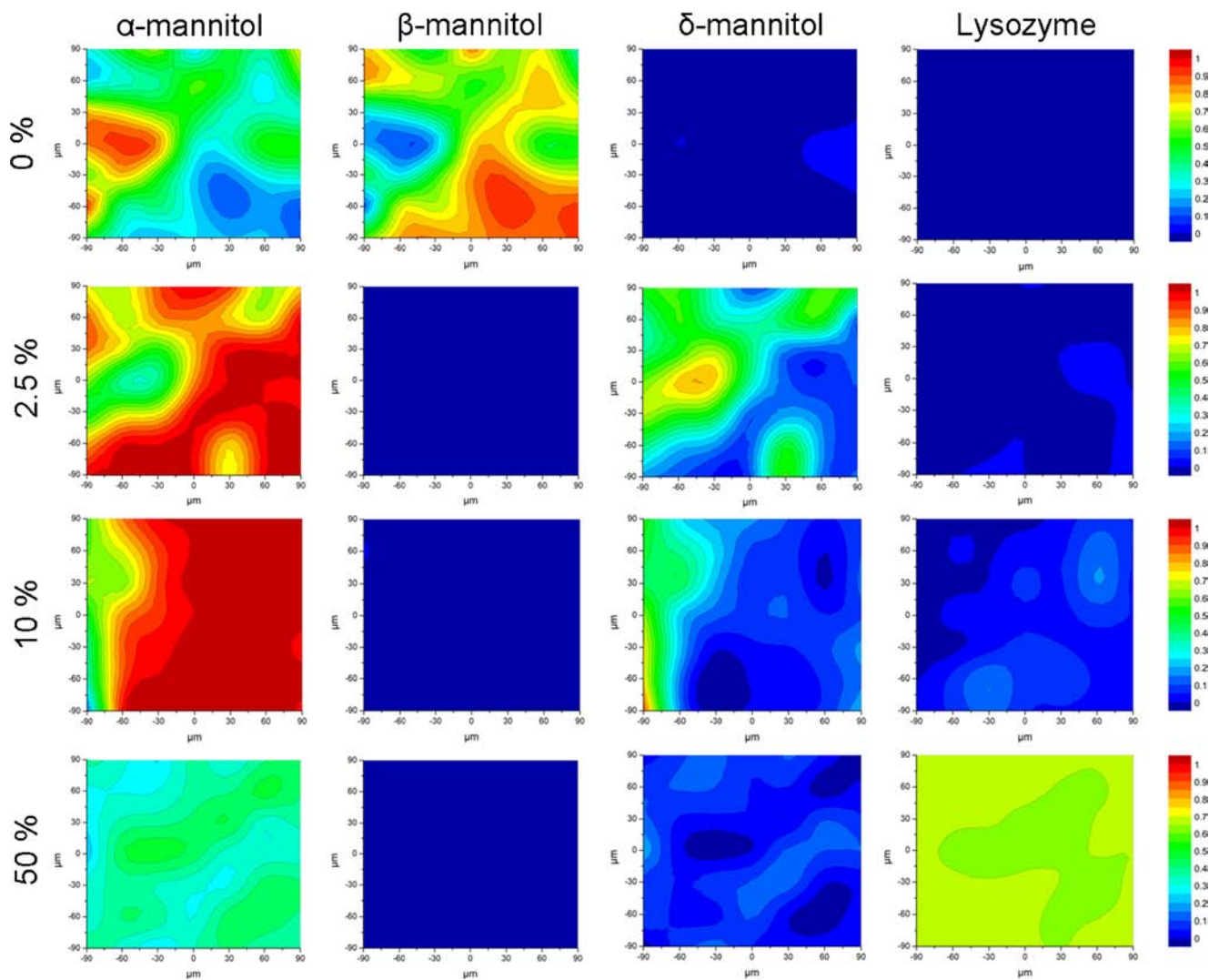


Fig. 7 The contour plots indicating the distribution of different mannitol forms and lysozyme content on the surface of single droplet levitation particles containing different nominal concentrations of the protein.

quantification (21–23). Furthermore, the signal arising from one component of the mixture might be hard to quantify, if there are overlapping reflections or the intensity is weak (24). Finally, the signal is obtained from a sufficiently large area of the powder sample without possibilities to focus to a specific spot and thus the method is not suitable for mapping or imaging. In contrary to XRPD, the different data collection principle of Raman spectroscopy allows spatial signal collection and thus it is suitable for surface characterization (25), which is the case in this current study. However, Raman spectroscopy can also be used in depth scanning due to the fact that the laser beam is focused to the sample through a microscope (25). Although some controversy has been proposed by Li *et al.* (26), as it seems that the vibrational spectroscopies, such as Raman spectroscopy, are able to produce more robust quantification models for polymorphic form determination than XRPD (21–23). This justifies the

quantification of different forms on the basis of Raman mapping and PLS-DA modeling.

The results showed that the XRPD diffractograms of spray-dried powder contained diffractions designating only mostly β -form and traces with α -form, when pure mannitol was spray dried. The diffractions indicate the presence only of β -form, when the lysozyme concentration was 2.5% (*w/w*), and the presence mostly of α -form and traces of β -form, when the protein concentration was 10% (*w/w*). According to XRPD there was only α form present, when the protein loading degree was 50% (*w/w*).

The results obtained by Raman mapping of spray dried powder are well in line with the XRPD results. There is only one exception: the formulation containing 2.5% (*w/w*) of lysozyme seems to have also some α -form, which could not be detected with XRPD. Furthermore, Fig. 3 shows that the distribution of different components on the spray dried

powder is very even. This can be due to the fact that the current spray-drying process resulted in fine particles and thus the distribution of different components could not be detected with the resolution used for mapping. The percentage of different mannitol polymorphs based on the quantitative estimations by Raman mapping and PLS-DA results, are presented in Table 1. In spray dried powder, β mannitol is the dominating form when protein concentration is 0 or 2.5% (w/w). With an increase in protein content, there seems to be more and more α form, and with the protein concentration of 50% (w/w) only α -mannitol is present. Hence the mannitol polymorphism from the spray-drying process in this study is in agreement with the findings in the previous study (9), even though different solid concentrations in the feed were used, i.e. a mixture of β -mannitol and α -mannitol were produced, and the ratio of α -mannitol to β -mannitol increased with an increase in lysozyme concentration.

In contrast to spray dried particles, the size of the single droplet levitation particles is much larger, which enables observation of the differentiation of the components with the resolution used for Raman mapping (Fig. 7). As with spray dried particles, the single droplet levitation particle that did not contain any protein consisted of both α and β mannitol, with the favor of the latter. However, δ form started to appear when protein was present (Fig. 7, Table 1), and its amount is clearly lower than the dominating α form. In addition with an increase in lysozyme concentration the ratios of α -mannitol to δ -mannitol are increased (Table 1). Interestingly, the protein seems to be found from the same location as α mannitol, when Fig. 7 is inspected, especially in the case of 10% (w/w) and 50% (w/w) formulation. This indicates that the protein is clearly affecting the polymorphic form of mannitol by inducing the formation of α form in the drying conditions similar to that used in the spray-drying process with Büchi Mini B-290 spray dryer. It is in agreement with that in the spray dried particles, α -mannitol become dominating with an increase in lysozyme in the formulations. The co-localization of α -mannitol and lysozyme suggests the presence of lysozyme favors inducing α -mannitol in the particles from the spray

drying process and DKA. As far as why δ -mannitol but not β -mannitol appears from the DKA process is not clear to us. DKA is much slower drying process (due to much larger initial droplet size) as compared to the spray drying process. One would expect that mannitol molecules might have longer time to arrange themselves to the most stable form, β -mannitol, instead of two metastable forms, i.e. α -mannitol and δ -mannitol. One possible reason behind this unexpected result could be that the acoustic energy might disrupt the formation of the most stable form of mannitol. However considering the acoustic frequency (i.e. ~ 55 kHz) used in the current DKA operation (14) i.e. β -mannitol, instead of two metastable forms, i.e. α -mannitol and δ -mannitol. One possible reason behind this unexpected result could be that the acoustic energy might disrupt the formation of the most stable form of mannitol. However considering the acoustic frequency (i.e. ~ 55 kHz) used in the current DKA operation (14) hardly believe this acoustic wave will be sufficient to induce nucleation and crystal growth, and result in different polymorphism. Another possible reason could be the interaction of lysozyme and mannitol interrupt mannitol molecules to the most stable solid state form, as it is known water replacement is one of the mechanisms behind stabilizing proteins with polyols. Nonetheless the use of DKA in the present study provided us the opportunity of investigating the mannitol polymorphism using Raman mapping. And Raman results suggested that the presence of lysozyme favored the appearance of α -mannitol in the particles from DKA evidenced by close proximity of lysozyme and mannitol in the particles. The mechanisms behind such molecular arrangement of lysozyme and mannitol under different drying processes *will need further investigation*. The current study underlines mannitol and protein interacts differently upon the different drying process. Compared to XRPD, Raman mapping together with PLS-DA might be able to provide more detailed information of the quantitative estimation of polymorphic forms.

CONCLUSION

In the presence of lysozyme, spray-dried mannitol particles consisted of a mixture of α -mannitol and β -mannitol, while a mixture of α -mannitol and δ -mannitol was found when the same formulations were processed with a drying kinetics analyzer. In addition, the ratios of α -mannitol to another solid state form, i.e. β -mannitol or δ -mannitol increased as a function of lysozyme in the formulation, indicating that this protein tended to induce the formation of α -mannitol under the drying condition used in this study. This was also evidenced by the co-localization of α -mannitol and lysozyme in the particles as found in the Raman mapping study. In combination with multivariate data analysis Raman microscopy provided

Table 1 The Percentage of Different Mannitol Polymorphs in Spray Dried Powder and Single Levitation Droplet Particles

Sample type	Mannitol form	Protein concentration % nw/w			
		0	2.5	10	50
Spray dried powder	α	6%	13%	79%	100%
	β	94%	87%	21%	–
	δ	–	–	–	–
Particles from DKA	α	40%	73%	83%	87%
	β	60%	–	–	–
	δ	–	27%	17%	13%

detailed spatially-resolved quantitative information of the solid state composition.

ACKNOWLEDGMENTS AND DISCLOSURES

Funding from The Danish Council for Technology and Innovation for the Innovation Consortium NanoMorph (952320/2009) is acknowledged. Erik Wisaeus (Danish Technology Institute) is acknowledged for his wonderful work on SEM. The grant from Lundbeckfonden for the purchase of X-ray powder diffractometer is acknowledged (grant decision 479/06). Erik Skibsted from Novo Nordisk A/S is acknowledged for his enthusiastic support with Raman mapping technique.

REFERENCES

1. Yoshinari T, Forbes RT, York P, Kawashima Y. Moisture induced polymorphic transition of mannitol and its morphological transformation. *Int J Pharm.* 2002;247:69–77.
2. Yang M, Yamamoto H, Kurashima H, Takeuchi H, Yokoyama T, Tsujimoto H, *et al.* Design and evaluation of inhalable chitosan-modified poly (DL-lactic-co-glycolic acid) nanocomposite particles. *Euro J Pharm Sci.* 2012;47:235–43.
3. Ingvarsson PT, Schmidt ST, Christensen D, Larsen NB, Hinrichs WL, Andersen P, *et al.* Designing CAF-adjuvanted dry powder vaccines: spray drying preserves the adjuvant activity of CAF01. *J Control Release.* 2013;167:256–64.
4. Owens DR, Zinman B, Bolli G. Alternative routes of insulin delivery. *Diabetic Med.* 2003;20:886–98.
5. Grohganz H, Gildemyn D, Skibsted E, Flink JM, Rantanen J. Rapid solid-state analysis of freeze-dried protein formulations using NIR and Raman spectroscopies. *J Pharm Sci.* 2011;100:2871–5.
6. Burger A, Henck JO, Hetz S, Rollinger JM, Weissnicht AA, Stottner H. Energy/temperature diagram and compression behavior of the polymorphs of d-mannitol. *J Pharm Sci.* 2000;89:457–68.
7. Nunes C, Suryanarayanan R, Botez CE, Stephens PW. Characterization and crystal structure of d-mannitol hemihydrate. *J Pharm Sci.* 2004;93:2800–9.
8. Costantino HR, Andya JD, Nguyen PA, Dasovich N, Sweeney TD, Shire SJ, *et al.* Effect of mannitol crystallization on the stability and aerosol performance of a spray-dried pharmaceutical protein, recombinant humanized anti-IgE monoclonal antibody. *J Pharm Sci.* 1998;87:1406–11.
9. Grohganz H, Lee YY, Rantanen J, Yang M. The influence of lysozyme on mannitol polymorphism in freeze-dried and spray-dried formulations depends on the selection of the drying process. *Int J Pharm.* 2013;447:224–30.
10. Hulse WL, Forbes RT, Bonner MC, Getrost M. Influence of protein on mannitol polymorphic form produced during co-spray drying. *Int J Pharm.* 2009;382:67–72.
11. Lee YY, Wu JX, Yang M, Young PM, van den Berg F, Rantanen J. Particle size dependence of polymorphism in spray-dried mannitol. *Eur J Pharm Sci.* 2011;44:41–8.
12. Schiffter H, Lee G. Single-droplet evaporation kinetics and particle formation in an acoustic levitator. Part 1: evaporation of water microdroplets assessed using boundary-layer and acoustic levitation theories. *J Pharm Sci.* 2007;96:2274–83.
13. Brask AT, Ullum PT, Andersen SK. High-temperature ultrasonic levitator for investigating drying kinetics of single droplets. The Proceedings of the 6th Intl. Conf. on Multiphase Flow, Leipzig, 9–13 July, 2007; paper No. 789.
14. Ullum, T, Sloth J, Brask A, Wahlberg M. CFD Simulation of a Spray Dryer Using an Empirical Drying Model, 16th International Drying Symposium (IDS2008), Hyderabad, India, 9–13 November, 2008; pp. 301–308.
15. Haaland DM, Thomas EV. Partial least-squares methods for spectral analyses. 1. Relation to other quantitative calibration methods and the extraction of qualitative information. *Anal Chem.* 1988;60:1193–202.
16. Wold S, Sjöström M, Eriksson L. PLS-regression: a basic tool of chemometrics. *Chemom Intell Lab Syst.* 2001;58:109–30.
17. Rinnan A, van den Berg F, Engelsen SB. Review of the most common pre-processing techniques for near-infrared spectra. *Trac Trend Anal Chem.* 2009;28:1201–22.
18. Sano Y, Keey RB. The drying of a spherical particle containing colloidal material into a hollow sphere. *Chem Eng Sci.* 1982;37(6): 881–9.
19. Ranz WE, Marshall WR. Evaporation from drops - part 1. *Chem Eng Prog.* 1952;48:141–6.
20. Ranz WE, Marshall WR. Evaporation from drops - part 2. *Chem Eng Prog.* 1952;48:173–80.
21. Tian F, Zhang F, Sandler N, Gordon KC, McGoverin CM, Strachan C, *et al.* Influence of sample characteristics on quantification of carbamazepine hydrate formation by X-ray powder diffraction and Raman spectroscopy. *Eur J Pharm Biopharm.* 2007;66:466–74.
22. Németh Z, Kis GC, Pokol G, Demeter Á. Quantitative determination of famotidine polymorphs: X-ray powder diffractometric and Raman spectrometric study. *J Pharm Biomed Anal.* 2009;49:338–46.
23. Croker DM, Hennigan MC, Maher A, Hu Y, Ryder AG, Hodnett BK. A comparative study of the use of powder X-ray diffraction, Raman and near infrared spectroscopy for quantification of binary polymorphic mixtures of paracetamol. *J Pharm Biomed Anal.* 2012;63:80–6.
24. Pikal MJ, Lukes AI, Lang JE, Gaines K. Quantitative crystallinity determinations of β -lactam antibiotics by solution calorimetry: Correlation and stability. *J Pharm Sci.* 1978;67:767–72.
25. Gordon KC, McGoverin CM. Raman mapping of pharmaceuticals. *Int J Pharm.* 2011;417(1–2):151–62.
26. Li Y, Chow PS, Tan RBH. Quantification of polymorphic impurity in an enantiotropic polymorphic system using differential scanning calorimetry, X-ray powder diffraction and Raman spectrometry. *Int J Pharm.* 2011;451:110–8.